Effects of Lovelock gravity on the Joule–Thomson expansion

Jie-Xiong Mo[1,2] and Gu-Qiang Li[1,2]

[1] Institute of Theoretical Physics, Lingnan Normal University, Zhanjiang 524048, Guangdong, People's Republic of China
[2] Department of Physics, Lingnan Normal University, Zhanjiang 524048, Guangdong, People's Republic of China

E-mail: mojiexiong@gmail.com

Abstract

Effects of Lovelock gravity on the Joule–Thomson expansion are probed from various perspectives. The well-known Joule–Thomson coefficient is derived with both the explicit expression and intuitive image presented. Moreover, the inversion curves showing the relation between the inversion temperature and the inversion pressure are studied. It is shown that for given inversion pressure, the inversion temperature of the case $\alpha \neq 0$ (α is the Lovelock parameter) is much lower than that of the case $\alpha = 0$. And the inversion temperature tends to decrease with α, in contrast to the effect of the electric charge. It is also shown that the ratio between the minimum inversion temperature and the critical temperature decreases with α for $\alpha \neq 0$. Furthermore, the isenthalpic curves are investigated with rich physics revealed. The intersection point between the isenthalpic curve and the inversion curve is exactly the inversion point discriminating the heating process from cooling process. It is shown that both the inversion temperature and the inversion pressure for $\alpha \neq 0$ are much lower for the same given mass of the black hole, showing the effect of Lovelock gravity. Last but not the least, we discuss the uncharged Lovelock AdS black holes. It is shown that the Joule–Thomson coefficient is always positive, suggesting the expansion is always in the regime of cooling process. And no inversion temperature exists, in contrast to the case $Q \neq 0$. Isenthalpic curves are also quite different since the temperature increases monotonically with the pressure when the mass is specified.

Keywords: Joule–Thomson expansion, black hole, Lovelock

(Some figures may appear in colour only in the online journal)

1. Introduction

Thermodynamics of AdS (Anti-de Sitter) black holes is such an exciting topic that has attracted lots of attention. It was disclosed that there exists phase transition between the Schwarzschild AdS black hole and the thermal AdS space [1]. And this transition was then named after its discoverer, Hawking and Page. Concerning charged AdS black holes, rich phase structures were found by Chamblin *et al* [2, 3]. It was shown that charged AdS black holes are closely related to the liquid-gas system. This observation was further supported by the study of $P - V$ criticality [4], which was carried out in the so-called extended phase space. In this framework, the cosmological constant is identified as the thermodynamic pressure and the mass should be interpreted as enthalpy [5]. Moreover, it was suggested recently that AdS black holes share many similarities with the ordinary thermodynamic systems in critical behavior [6–8]. One can refer to the most recent review [9] for details and more references. Apart from the critical phenomena, many other interesting aspects of AdS black holes have also been covered in the recent literatures. For example, the novel concept of holographic heat engine was proposed by Johnson [10], suggesting one more way to extract mechanical work from black holes. This idea was further generalized with the proposal that one can even implement black holes as efficient power plant [11].

Recently, Joule–Thomson expansion, a well-known process in classical thermodynamics, was generalized to AdS black holes by Ökcü and Aydiner [12] creatively. For RN-AdS black holes [12] and Kerr–AdS black holes [13], both the inversion curves and isenthalpic curves were investigated. These pioneer works were generalized to quintessence RN-AdS Black Holes [14], holographic superfluids [15], Gauss–Bonnet gravity [16] and RN-AdS black holes in $f(R)$ gravity [17]. More recently, we probed in detailed the effect of the dimensionality on the Joule–Thomson expansion [18]. It was shown that [18] the ratio between minimum inversion temperature and the critical temperature decreases with the dimensionality d while it recovers the result in [12] when $d = 4$.

We are curious to examine our former result in another high-dimensional space-time. On the other hand, we are also interested in the effect of Lovelock gravity on the Joule–Thomson expansion. So we choose our target as seven-dimensional Lovelock AdS black holes. Lovelock gravity [19] successfully solved the problems of ghosts [20] and field equations of fourth order. So it is certainly of interest to probe the black hole solutions and their thermodynamics within the framework of Lovelock gravity [21–56]. Dehghani *et al* [21] found the topological black hole solutions in Lovelock–Born–Infeld gravity. Their thermodynamics and critical behavior were investigated in detail [22–30]. Kastor *et al* [31] presented an explicit formula for the ADM mass and free energy of AdS black holes in Lovelock gravity and studied the Hawking–Page phase transition. In this paper, we would like to generalize the current research of Joule–Thomson expansion to the black hole solutions found in [21]. This generalization is of physical significance since varieties of intriguing thermodynamic properties have been disclosed for this solution. It is naturally expected that the research in this paper may give rise to novel findings concerning the Joule–Thomson expansion. To concentrate on the effect of Lovelock gravity, we do not consider the nonlinear electromagnetic filed here.

The organization of this paper is as follows. Section 2 devotes to a short review of the thermodynamics of $(n + 1)$-dimensional Lovelock AdS black holes. In section 3, we will probe the Joule–Thomson expansion of seven-dimensional Lovelock AdS black holes. Conclusion will be presented in section 4.

2. A brief review of the thermodynamics of ($n+1$)-dimensional Lovelock AdS black holes

The action of Lovelock gravity coupled with Born–Infeld electromagnetic filed can be written as [21]

$$I_G = \frac{1}{16\pi} \int \mathrm{d}^{n+1}x\sqrt{-g}\big(-2\Lambda + \mathcal{L}_1 + \alpha_2\mathcal{L}_2 + \alpha_3\mathcal{L}_3 + L(F)\big), \tag{1}$$

where

$$\mathcal{L}_1 = R, \tag{2}$$

$$\mathcal{L}_2 = R_{\mu\nu\gamma\delta}R^{\mu\nu\gamma\delta} - 4R_{\mu\nu}R^{\mu\nu} + R^2, \tag{3}$$

$$\begin{aligned}
\mathcal{L}_3 = {}& 2R^{\mu\nu\sigma\kappa}R_{\sigma\kappa\rho\tau}R^{\rho\tau}{}_{\mu\nu} + 8R^{\mu\nu}{}_{\sigma\rho}R^{\sigma\kappa}{}_{\nu\tau}R^{\rho\tau}{}_{\mu\kappa} + 24R^{\mu\nu\sigma\kappa}R_{\sigma\kappa\nu\rho}R^{\rho}{}_{\mu} \\
& + 3RR^{\mu\nu\sigma\kappa}R_{\sigma\kappa\mu\nu} + 24R^{\mu\nu\sigma\kappa}R_{\sigma\mu}R_{\kappa\nu} + 16R^{\mu\nu}R_{\nu\sigma}R^{\sigma}{}_{\mu} \\
& - 12RR^{\mu\nu}R_{\mu\nu} + R^3,
\end{aligned} \tag{4}$$

$$L(F) = 4\beta^2\left(1 - \sqrt{1 + \frac{F^2}{2\beta^2}}\right). \tag{5}$$

$\mathcal{L}_1$, $\mathcal{L}_2$, $\mathcal{L}_3$ and $L(F)$ represent the Einstein–Hilbert Lagrangian, Gauss–Bonnet Lagrangian, the third order Lovelock Lagrangian and Born–Infeld Lagrangian respectively with α_2, α_3 denoting the second and third order Lovelock coefficients and β denoting the Born–Infeld parameter.

Dehghani *et al* [21] derived its ($n+1$)-dimensional black hole solution as

$$\mathrm{d}s^2 = -f(r)\mathrm{d}t^2 + \frac{\mathrm{d}r^2}{f(r)} + r^2\mathrm{d}\Omega^2, \tag{6}$$

where

$$f(r) = k + \frac{r^2}{\alpha}[1 - g(r)^{1/3}], \tag{7}$$

$$g(r) = 1 + \frac{3\alpha m}{r^n} - \frac{12\alpha\beta^2}{n(n-1)}\left[1 - \sqrt{1+\eta} - \frac{\Lambda}{2\beta^2} + \frac{(n-1)\eta}{(n-2)}F(\eta)\right]. \tag{8}$$

$F(\eta)$ denotes the hypergeometric function $_2F_1\left(\left[\frac{1}{2}, \frac{n-2}{2n-2}\right], \left[\frac{3n-4}{2n-2}\right], -\eta\right)$ with $\eta = \frac{(n-1)(n-2)q^2}{2\beta^2 r^{2n-2}}$. It should be noted that this solution was obtained with the assumption that $\alpha_2 = \frac{\alpha}{(n-2)(n-3)}$, $\alpha_3 = \frac{\alpha^2}{72\binom{n-2}{4}}$ [21], where α denotes the Lovelock parameter.

In the above solution, m and q are parameters related to the mass M and the electric charge Q as

$$M = \frac{(n-1)\Sigma_k}{16\pi}m, \tag{9}$$

$$Q = \frac{\Sigma_k}{4\pi}\sqrt{\frac{(n-1)(n-2)}{2}}q. \tag{10}$$

Here, Σ_k denotes the volume of the $(n-1)$-dimensional hypersurface with constant curvature $(n-1)(n-2)k$ whose line element is represented by $d\Omega^2$ in the above metric. Note that the horizon radius r_+ is the largest root of the equation $f(r_+) = 0$. Then the mass can be expressed into the function of r_+.

Since we need to concentrate on the effect of Lovelock gravity, the effect of nonlinear electromagnetic filed can be excluded by considering the limit $\beta \to \infty$. Then

$$g(r) \to 1 + \frac{3\alpha m}{r^n} + \frac{6\alpha\Lambda}{n(n-1)} - \frac{3\alpha q^2}{r^{2n-2}}. \tag{11}$$

The mass, the Hawking temperature, the entropy and the electric potential Φ of topological Lovelock AdS black holes was derived as [21]

$$M = \frac{\Sigma_k}{48n\pi r_+^{n+6}}\{3n(n-1)q^2 r_+^8 + r_+^{2n}\left[kn(n-1)(3r_+^4 + 3kr_+^2\alpha + k^2\alpha^2) - 6r_+^6\Lambda\right]\}. \tag{12}$$

$$T = \frac{1}{12\pi(n-1)r_+(r_+^2 + k\alpha)^2}\{-6\Lambda r_+^6 - 3(n-2)(n-1)q^2 r_+^{8-2n}$$
$$+ (n-1)k[3(n-2)r_+^4 + 3(n-4)k\alpha r_+^2 + (n-6)k^2\alpha^2]\}. \tag{13}$$

$$S = \int_0^{r_+} \frac{1}{T}\left(\frac{\partial M}{\partial r_+}\right) dr = \frac{\Sigma_k(n-1)r_+^{n-5}}{4}\left(\frac{r_+^4}{n-1} + \frac{2kr_+^2\alpha}{n-3} + \frac{k^2\alpha^2}{n-5}\right), \tag{14}$$

$$\Phi = \frac{4\pi Q}{(n-2)r_+^{n-2}\Sigma_k}. \tag{15}$$

The integration in equation (14) is divergent for $n \leqslant 5$. And it is just the manifestation of the fact that the third order Lovelock gravity is non-trivial only for $n > 5$.

Treating the cosmological constant as a variable, the thermodynamic pressure and thermodynamic volume can be defined as [5]

$$P = -\frac{\Lambda}{8\pi}, \quad V = \left(\frac{\partial M}{\partial P}\right) = \frac{r_+^n \Sigma_k}{n}. \tag{16}$$

3. Joule–Thomson expansion of seven-dimensional Lovelock AdS black holes

In classical thermodynamics, Joule–Thomson expansion describes such an isenthalpic process in a thermally insulated tube that the gas expands from a high pressure section to a low pressure section through a porous plug. This process is also called throttling process and is widely applied in thermal machines such as air conditioner, liquefiers and heat pumps. Obviously, during this process the pressure decreases. And the expansion can be divided into the cooling process (the change of temperature is negative) and the heating process (the change of temperature is positive), which can be discriminated by an important criteria named as the Joule–Thomson coefficient. The coefficient can be defined as

$$\mu = \left(\frac{\partial T}{\partial P}\right)_H \tag{17}$$

where $\mu > 0$ corresponds to the cooling process while $\mu < 0$ corresponds to heating process. For more detailed information concerning the Joule–Thomson expansion of the real gas, one can refer to any textbook of classical thermodynamics or the nice review presented in [12].

3.1. The Joule–Thomson coefficient

Now we utilize the first law of black hole thermodynamics to derive the Joule–Thomson coefficient for Lovelock AdS black holes. The first law of black hole thermodynamics of seven-dimensional Lovelock AdS black holes in the extended phase space reads [26, 32]

$$\mathrm{d}H = T\mathrm{d}S + \Phi\mathrm{d}Q + V\mathrm{d}P + \mathcal{A}\mathrm{d}\alpha, \tag{18}$$

where $\mathcal{A}$ denotes the quantities conjugated to the Lovelock parameter. Note that the mass of the black hole is interpreted as the enthalpy in the extended phase space and the term $\mathcal{B}\mathrm{d}\beta$ is omitted here because the nonlinear electromagnetic field is not taken into account here.

From equation (18), one can obtain

$$0 = T\left(\frac{\partial S}{\partial P}\right)_H + V. \tag{19}$$

The conditions $\mathrm{d}H = 0, \mathrm{d}Q = 0, \mathrm{d}\alpha = 0$ have been used in the above derivation. On the other hand, the entropy S can be viewed as the function of the Hawking temperature T, the pressure P, the charge Q and the Lovelock parameter α. And one can express $\mathrm{d}S$ as

$$\mathrm{d}S = \left(\frac{\partial S}{\partial P}\right)_{T,\alpha,Q}\mathrm{d}P + \left(\frac{\partial S}{\partial T}\right)_{P,\alpha,Q}\mathrm{d}T + \left(\frac{\partial S}{\partial \alpha}\right)_{T,P,Q}\mathrm{d}\alpha + \left(\frac{\partial S}{\partial Q}\right)_{T,P,\alpha}\mathrm{d}Q, \tag{20}$$

from which one can further derive

$$\left(\frac{\partial S}{\partial P}\right)_H = \left(\frac{\partial S}{\partial P}\right)_{T,\alpha,Q} + \left(\frac{\partial S}{\partial T}\right)_{P,\alpha,Q}\left(\frac{\partial T}{\partial P}\right)_H. \tag{21}$$

Here, we have utilized $\mathrm{d}Q = 0, \mathrm{d}\alpha = 0$ again.

Substituting equation (17) into (21), one can obtain

$$\mu = \frac{1}{T\left(\frac{\partial S}{\partial T}\right)_{P,\alpha}}\left[-T\left(\frac{\partial S}{\partial P}\right)_{T,\alpha,Q} - V\right] = \frac{1}{C_{P,\alpha}}\left[T\left(\frac{\partial V}{\partial T}\right)_{P,\alpha,Q} - V\right]. \tag{22}$$

Note that both the Maxwell relation and the definition of specific heat have been applied.

One can also follow the approach proposed in [13] and derive the Joule–Thomson coefficient utilizing both the first law of black hole thermodynamics and the differentiation of the Smarr formula. We have shown in [18] both approaches are consistent with each other.

From equations (13), (14), (16) and (22), the explicit expression of μ for seven-dimensional Lovelock AdS black holes can be obtained as

$$\mu = \frac{2r_+^5\{r_+^6[40P\pi r_+^6 + 75r_+^2\alpha + 25\alpha^2 + r_+^4(70 + 8P\pi\alpha)] - 10q^2(15r_+^2 + 11\alpha)\}}{15(r_+^2 + \alpha)^3(10r_+^8 + 8P\pi r_+^{10} + 5\alpha r_+^6 - 10q^2)}. \tag{23}$$

The behavior of μ is depicted in figure 1 with the help of equation (23). Both a divergent point and a zero point can be observed in each subgraph. The horizon radius corresponding to the zero point (We use the notation r_{+i} to denote this horizon radius while the subscript i is short for 'inversion' in this paper) tends to decrease with the Lovelock parameter α. So does the
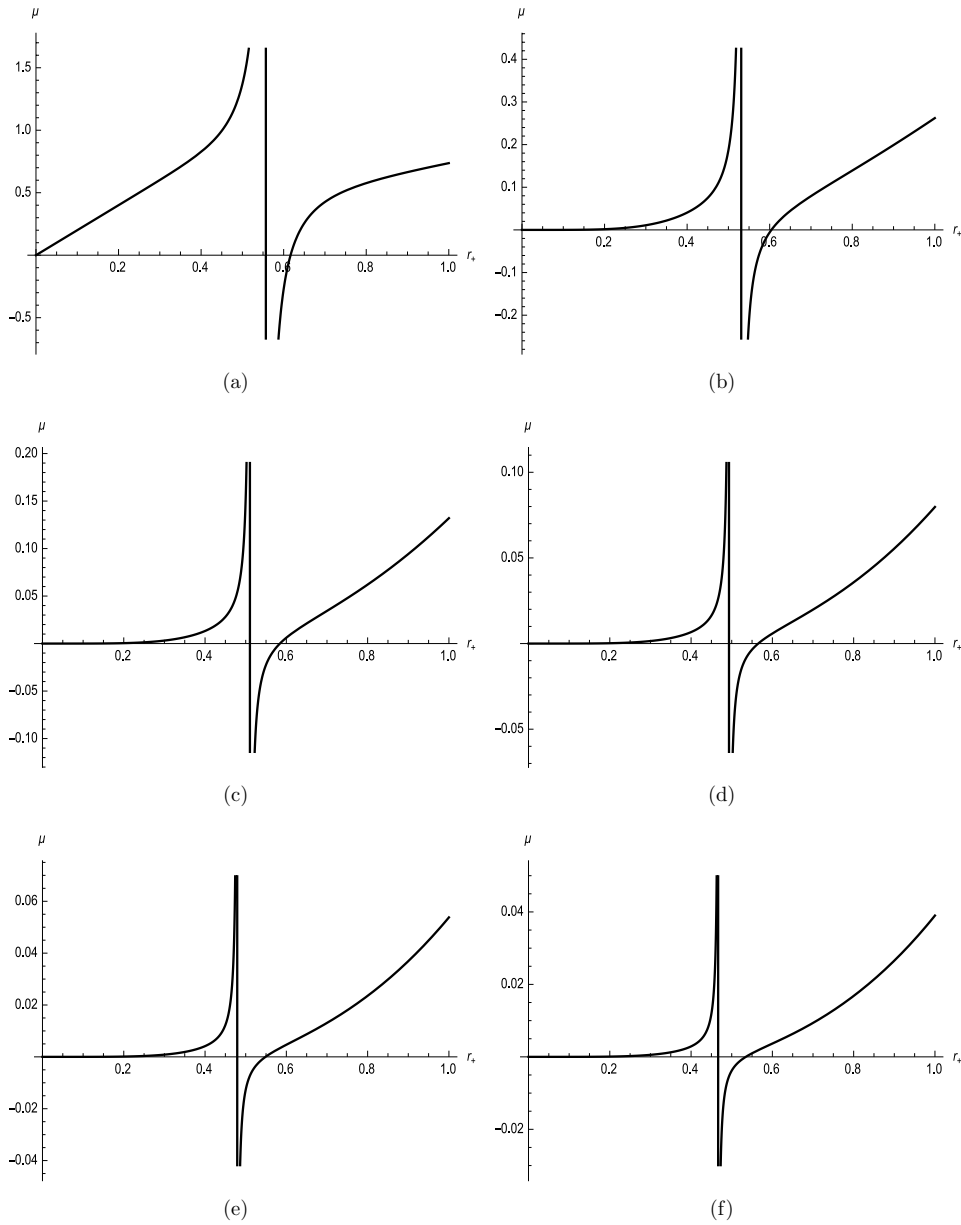
Figure 1. Joule–Thomson coefficient μ for $P = 1, Q = 1$ (a) $\alpha = 0$ (b) $\alpha = 0.5$ (c) $\alpha = 1.0$ (d) $\alpha = 1.5$ (e) $\alpha = 2.0$ (f) $\alpha = 2.5$.

horizon radius corresponding to the divergent point of μ. Remind that the divergent point of Joule–Thomson coefficient coincides with the zero point of Hawking temperature.

Utilizing equation (13), one can further obtain the inversion temperature T_i when P, Q, α is given. Inversion temperature is an important quantity to probe the Joule–Thomson expansion. In the following subsection, we will study the inversion curves which show the relation between the inversion temperature T_i and the inversion pressure P_i intuitively.

3.2. The inversion curves and the isenthalpic curves

As can be observed from the numerator of the righthand side of equation (23), the inversion pressure P_i and the corresponding r_{+i} satisfy

$$r_{+i}^6[40P_i\pi r_{+i}^6 + 75r_{+i}^2\alpha + 25\alpha^2 + r_{+i}^4(70 + 8P_i\pi\alpha)] - 10q^2(15r_{+i}^2 + 11\alpha) = 0. \tag{24}$$

Via equations (13), (16) and (24), the inversion curves are plotted in figure 2. For $\alpha = 0.5$, figure 2(a) shows the effect of the electric charge on the inversion curves. With the increasing of Q, the inversion temperature for given pressure tends to increase. This behavior is qualitatively similar to the RN-AdS black holes [12]. Figure 2(b) further compares the inversion curve of the case $\alpha = 0.5$ with that of the case $\alpha = 0$. Although in both case the inversion temperature T_i increases with the inversion pressure P_i, the slope is rather different. For given P_i, the inversion temperature of the case $\alpha = 0.5$ is much lower. To further probe the effect of the Lovelock gravity on the inversion curves, figures 2(c) and (d) shows the inversion curves for different α while Q is chosen to be 1 and 2 respectively. As can be witnessed in these two sub-figures, T_i tends to decrease with α for given P_i, in contrast to the effect of the electric charge.

Since T_i increases monotonically with P_i, there exists a minimum inversion temperature $T_{\min}$ which can be calculated by demanding $P_i = 0$. The ratio between $T_{\min}$ and the critical temperature T_c is of potential interest. It was shown that this ratio is 1/2 for four-dimensional charged AdS black holes [12] and Kerr–AdS black holes [13] but tends to decrease with the dimensionality d [18]. The results of the ratio $T_{\min}/T_c$ for various α is shown in table 1. For $\alpha = 0$, it recovers the value of $d = 7$ [18]. For $\alpha \neq 0$, the ratio decreases with α. Note that there is no analytic expression for the minimum inversion temperature due to the complexity of the equation of equation (24) and we had to present the numerical results here.

Apart from the inversion curves, the isenthalpic curves are also of interest considering Joule–Thomson expansion is an isenthalpic process. Within the framework of the extended phase space, the mass is interpreted as enthalpy [5]. Then isenthalpic curves can be plotted provided the mass of the black holes is fixed. Utilizing equations (12), (13) and (16), the isenthalpic curves for $\alpha = 0$ and $\alpha \neq 0$ is shown in figure 3. The inversion curves are shown together to gain a deeper understanding of the Joule–Thomson expansion. Each isenthalpic curve is divided into two branches by the inversion curve. The branch above the inversion curve represents the cooling process while the branch below the inversion curve represents the heating process. Note that the intersection point between the isenthalpic curve and the inversion curve is exactly the inversion point. So the inversion point discriminates the heating process from cooling process. Moreover, the inversion point is the maximum point for a specific isenthalpic curve, implying that during the whole Joule–Thomson expansion process the temperature is highest at the inversion point.

One can read off the inversion temperature and the inversion pressure from the intersection point between the isenthalpic curve and the inversion curve. Comparing the isenthalpic curves for $\alpha \neq 0$ with those of the case $\alpha = 0$, it can be witnessed that both T_i and P_i for $\alpha \neq 0$ are much lower for the same given mass of the black hole, showing the effect of Lovelock gravity. Moreover, we list the corresponding T_i and P_i for various mass in table 2. As M increases, both T_i and P_i increase, suggesting that the inversion temperature is higher for the Joule–Thomson expansion with a larger enthalpy.
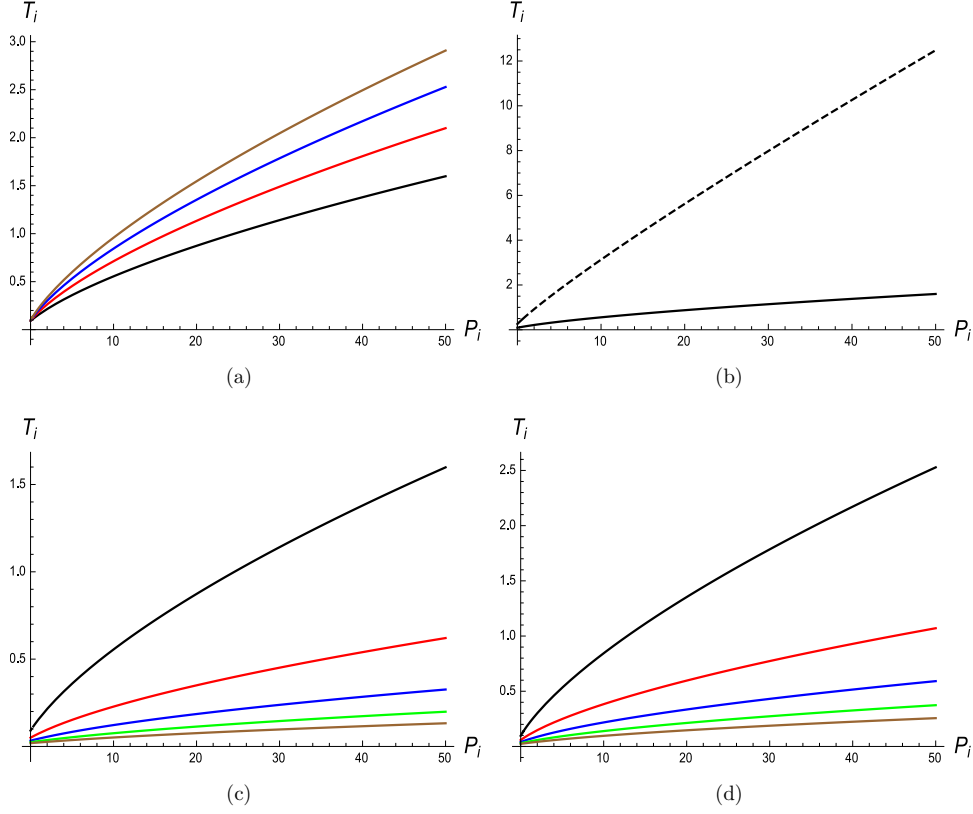
Figure 2. (a)The inversion curves for $\alpha = 0.5$. From top to bottom the curves correspond to $Q = 2.5$, $Q = 2.0$, $Q = 1.5$, $Q = 1.0$ respectively. (b) The inversion curves for $Q = 1$. The dashed line represents $\alpha = 0$ while the solid line represents $\alpha = 0.5$. (c) The inversion curves for $Q = 1$. From top to bottom the curves correspond to $\alpha = 0.5$, $\alpha = 1.0$, $\alpha = 1.5$, $\alpha = 2.0$, $\alpha = 2.5$ respectively. (d) The inversion curves for $Q = 2$. From top to bottom the curves correspond to $\alpha = 0.5$, $\alpha = 1.0$, $\alpha = 1.5$, $\alpha = 2.0$, $\alpha = 2.5$ respectively.

Table 1. $T_{\min}/T_{\mathrm{c}}$ of seven-dimensional charged Lovelock AdS black holes for various α ($Q = 1$).

α	0	0.5	1.0	1.5	2.0	2.5
$T_{\min}$	0.257949	0.090899	0.050021	0.033123	0.024259	0.018915
T_{c}	0.587673	0.200981	0.142337	0.116228	0.100658	0.090031
$T_{\min}/T_{\mathrm{c}}$	0.438933	0.452277	0.351427	0.284983	0.241004	0.210094

3.3. The uncharged case

Here, we consider the uncharged Lovelock AdS black holes. From equations (13), (14), (16) and (22), one can obtain the explicit expression of μ as
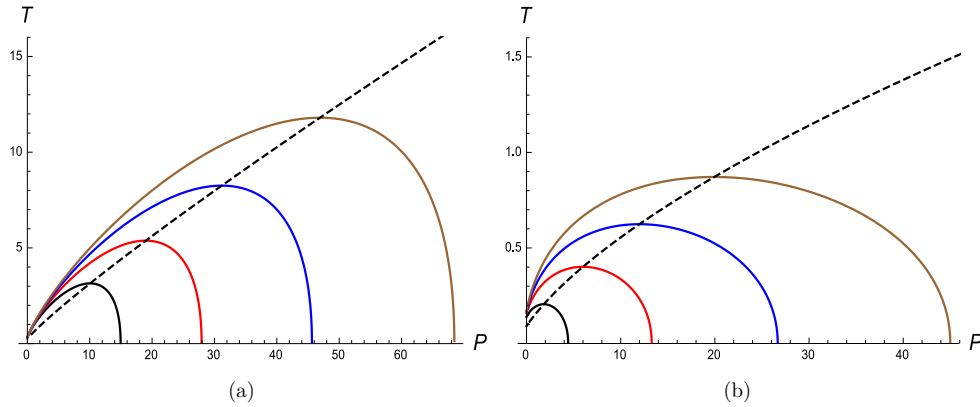
Figure 3. Isenthalpic curves for $Q = 1$ (a) $\alpha = 0$ (b) $\alpha \neq 0$ ($\alpha = 0.5$). In both graphs the curves from left to right correspond to $M = 2.0$, $M = 2.5$, $M = 3.0$, $M = 3.5$ respectively. Note that the inversion curve for $Q = 1$ is also depicted in both graphs via the dashed line.

Table 2. Inversion temperature and inversion pressure of seven-dimensional charged Lovelock AdS black holes for various mass ($Q = 1$).

α	M	P_i	T_i
0	2.0	9.99	3.13
0	2.5	19.04	5.39
0	3.0	31.17	8.26
0	3.5	47.02	11.77
0.5	2.0	1.70	0.21
0.5	2.5	5.95	0.40
0.5	3.0	11.94	0.63
0.5	3.5	19.87	0.87

$$\mu = \frac{2r_+^5 \left[40P\pi r_+^6 + 75r_+^2 \alpha + 25\alpha^2 + r_+^4 (70 + 8P\pi\alpha) \right]}{15(r_+^2 + \alpha)^3 (10r_+^2 + 8P\pi r_+^4 + 5\alpha)}. \tag{25}$$

As can be observed from above, both its numerator and denominator are always positive since $P > 0, \alpha \geqslant 0$. So there will be no zero point or divergent point for μ. This conclusion can also be confirmed in figure 4, where the behavior of μ is plotted for the case $Q = 0$ for various choices of α. μ is always positive, suggesting the expansion is always in the regime of cooling process. Then no inversion temperature exists in this case, in contrast to the case $Q \neq 0$. Isenthalpic curves are presented in figure 5 for both the case $\alpha = 0$ and $\alpha \neq 0$. It is shown in both cases that the temperature increases monotonically with the pressure when the mass is specified. This phenomenon is also quite different from that in the isenthalpic curves of $Q \neq 0$. It can be attributed to the observation that the system does not quite behave like a real (Van der Waals) gas in absence of charge and rotation .
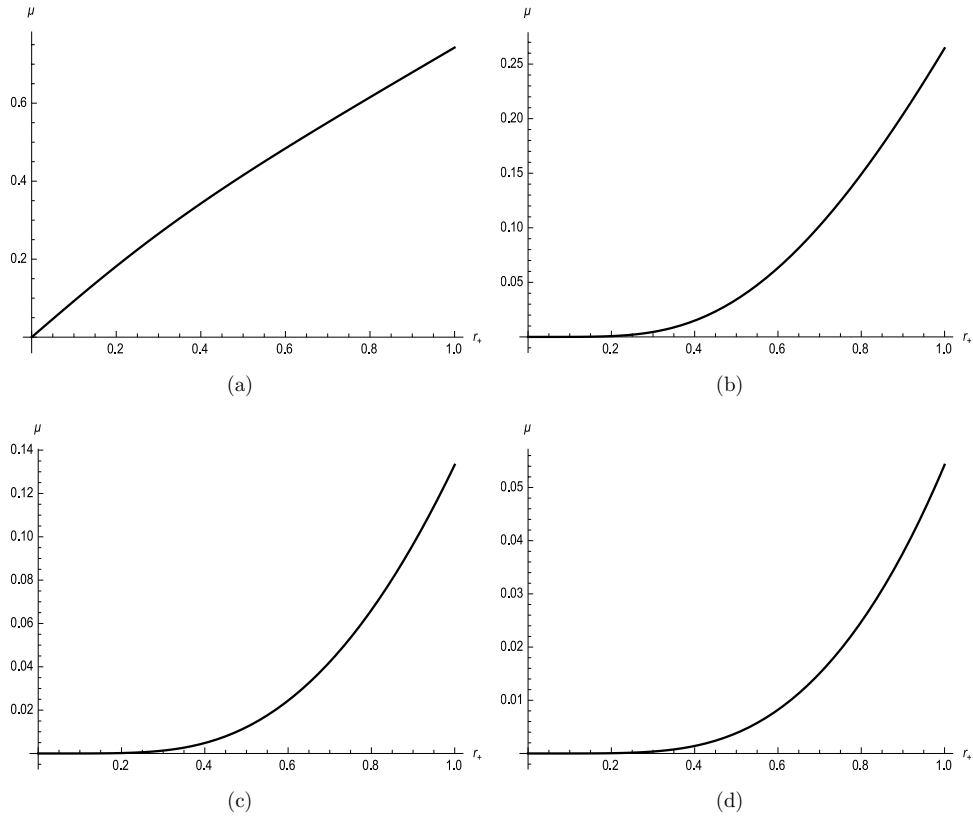
Figure 4. Joule–Thomson coefficient μ for $P = 1, Q = 0$ (a) $\alpha = 0$ (b) $\alpha = 0.5$ (c) $\alpha = 1.0$ (d) $\alpha = 2.0$.
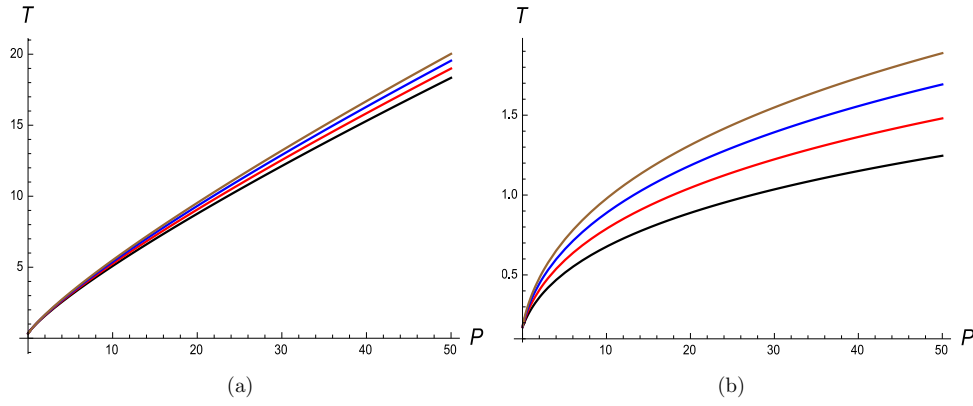

Figure 5. Isenthalpic curves for $Q = 0$ (a) $\alpha = 0$ (b) $\alpha \neq 0$ ($\alpha = 0.5$). In both graphs the curves from bottom to top correspond to $M = 2.0$, $M = 2.5$, $M = 3.0$, $M = 3.5$ respectively.

4. Conclusions

Effects of Lovelock gravity on the Joule–Thomson expansion is probed in this paper from various perspectives. Specifically, we investigate the Joule–Thomson expansion of seven-dimensional Lovelock AdS black holes.

Firstly, the well-known Joule–Thomson coefficient μ is derived via the first law of black hole thermodynamics. The explicit expression of μ is obtained while its behavior is also shown intuitively. Both a divergent point and a zero point exist. Here, the divergent point corresponds to the zero point of Hawking temperature while the zero point is the inversion point that discriminate the cooling process from heating process. It is shown that the horizon radius corresponding to the zero point tends to decrease with the Lovelock parameter α. So does the horizon radius corresponding to the divergent point of μ. This suggests that the effect of Lovelock gravity decreases the horizon radius of the black hole that changes between the heating process and the cooling process.

Secondly, the inversion curves showing the relation between the inversion temperature and the inversion pressure are studied. With the increasing of Q, the inversion temperature for given pressure tends to increase. This behavior is qualitatively similar to the RN-AdS black holes. Comparing the inversion curve of the case $\alpha \neq 0$ with that of the case $\alpha = 0$, it is shown that in both case the inversion temperature T_i increases with the inversion pressure P_i. However, the slope is rather different. For given P_i, the inversion temperature of the case $\alpha \neq 0$ is much lower. Moreover, the inversion temperature tends to decrease with α for given P_i, in contrast to the effect of the electric charge. We also probe the ratio between $T_{\min}$ and the critical temperature T_c. It is shown that the ratio $T_{\min}/T_c$ decreases with α for $\alpha \neq 0$ while it recovers the result in former literature [18] for $\alpha = 0$. These observation suggests that the effect of Lovelock gravity makes the inversion much easier (lower inversion temperature), which can be further understood considering the fact that gravity becomes weaker with increase in Lovelock order.

Thirdly, the isenthalpic curves are investigated with rich physics revealed. Each isenthalpic curve is divided into two branches by the inversion curve. The branch above the inversion curve represents the cooling process while the branch below the inversion curve represents the heating process. And the intersection point between the isenthalpic curve and the inversion curve is exactly the inversion point. So the inversion point discriminates the heating process from cooling process. Moreover, the inversion point is the maximum point for a specific isenthalpic curve, implying that during the whole Joule–Thomson expansion process the temperature is highest at the inversion point. One can read off the inversion temperature and the inversion pressure from the intersection point between the isenthalpic curve and the inversion curve. Comparing the case $\alpha \neq 0$ with the case $\alpha = 0$, it can be witnessed that both T_i and P_i for $\alpha \neq 0$ are much lower for the same given mass of the black hole, showing the effect of Lovelock gravity. This result also supports the finding that the effect of Lovelock gravity makes the inversion much easier. One can interpret this finding by considering the fact that gravity becomes weaker with increase in Lovelock order. Moreover, both T_i and P_i increase as M increases, suggesting that the inversion temperature is higher for the Joule–Thomson expansion with a larger enthalpy.

Last but not the least, the uncharged Lovelock AdS black holes are discussed. It is shown that μ is always positive, suggesting the expansion is always in the regime of cooling process. Then no inversion temperature exists in this case, in contrast to the case $Q \neq 0$. Isenthalpic curves are also quite different from those of $Q \neq 0$. It is shown for both the cases $\alpha \neq 0$ and $\alpha = 0$ that the temperature increases monotonically with the pressure when the mass is specified.

For future directions, one can further probe the combined effects of both the Lovelock gravity and the Born–Infeld field on the Joule–Thomson expansion based on the metric and results in this paper. Recently, an interesting phenomenon was reported [57, 58] that the isenthalpic curve does not intersect with the inversion curve beyond a certain value of charge and the system is always in the heating phase. One can also search for this phenomenon within the framework of Lovelock gravity.

Acknowledgments

ORCID iDs

Jie-Xiong Mo ⬤ https://orcid.org/0000-0002-8527-4005

References

[1] Hawking S W and Page D N 1983 Thermodynamics of black holes in Anti-de Sitter space *Commun. Math. Phys.* **87** 577
[2] Chamblin A, Emparan R, Johnson C V and Myers R C 1999 Charged AdS black holes and catastrophic holography *Phys. Rev.* D **60** 064018
[3] Chamblin A, Emparan R, Johnson C V and Myers R C 1999 Holography, thermodynamics and fluctuations of charged AdS black holes *Phys. Rev.* D **60** 104026
[4] Kubizňák D and Mann R B 2012 $P - V$ criticality of charged AdS black holes *J. High Energy Phys.* JHEP07(2012)033
[5] Kastor D, Ray S and Traschen J 2009 Enthalpy and the mechanics of AdS black holes *Class. Quantum Grav.* **26** 195011
[6] Gunasekaran S, Mann R B and Kubizňák D 2012 Extended phase space thermodynamics for charged and rotating black holes and Born–Infeld vacuum polarization *J. High Energy Phys.* JHEP11(2012)110
[7] Altamirano N, Kubizňák D and Mann R B 2013 Reentrant phase transitions in rotating Anti de Sitter black holes *Phys. Rev.* D **88** 101502
[8] Altamirano N, Kubizňák D, Mann R B and Sherkatghanad Z 2014 Kerr–AdS analogue of triple point and solid/liquid/gas phase transition *Class. Quantum Grav.* **31** 042001
[9] Kubizňák D, Mann R B and Teo M 2017 Black hole chemistry: thermodynamics with lambda *Class. Quantum Grav.* **34** 063001
[10] Johnson C V 2014 Holographic heat engines *Class. Quantum Grav.* **31** 205002
[11] Wei S W and Liu Y X 2019 Implementing black hole as efficient power plant *Commun. Theor. Phys.* **71** 711
[12] ökcü ö and Aydiner E 2017 Joule–Thomson expansion of the charged AdS black holes *Eur. Phys. J. C* **77** 24
[13] ökcü ö and Aydiner E 2018 Joule–Thomson expansion of Kerr–AdS black holes *Eur. Phys. J. C* **78** 123

[14] Ghaffarnejad H, Yaraie E and Farsam M 2018 Quintessence Reissner Nordström Anti de Sitter black holes and Joule Thomson effect *Int. J. Theor. Phys.* **57** 1671–82

[15] D'Almeida R and Yogendran K P 2018 Thermodynamic properties of holographic superfluids (arXiv:1802.05116)

[16] Lan S Q 2018 Joule–Thomson expansion of charged Gauss–Bonnet black holes in AdS space *Phys. Rev.* D **98** 084014

[17] Chabab M, El Moumni H, Iraoui S, Masmar K and Zhizeh S 2018 Joule–Thomson expansion of RN-AdS black holes in $f(R)$ gravity *Lett. High Energy Phys.* **02** 05

[18] Mo J X, Li G Q, Lan S Q and Xu X B 2018 Joule–Thomson expansion of d-dimensional charged AdS black holes *Phys. Rev.* D **98** 124032

[19] Lovelock D 1971 The Einstein tensor and its generalizations *J. Math. Phys., NY* **12** 498

[20] Boulware D G and Deser S 1985 String-generated gravity models *Phys. Rev. Lett.* **55** 2656

[21] Dehghani M H, Alinejadi N and Hendi S H 2008 Topological black holes in Lovelock–Born–Infeld gravity *Phys. Rev.* D **77** 104025

[22] Zou D, Yue R and Yang Z 2011 Thermodynamics of third order Lovelock Anti-de Sitter black holes revisited *Commun. Theor. Phys.* **55** 449–56

[23] Li P, Yue R H and Zou D C 2011 Thermodynamics of third order Lovelock–Born–Infeld black holes *Commun. Theor. Phys.* **56** 845–50

[24] Lala A 2013 Critical phenomena in higher curvature charged AdS black holes *Adv. High Energy Phys.* **2013** 918490

[25] Mo J X and Liu W B 2015 Non-extended phase space thermodynamics of Lovelock AdS black holes in the grand canonical ensemble *Eur. Phys. J.* C **75** 211

[26] Mo J X and Liu W B 2014 $P - V$ criticality of topological black holes in Lovelock–Born–Infeld gravity *Eur. Phys. J.* C **74** 2836

[27] Belhaj A, Chabab M, EL Moumni H, Masmar K and Sedra M B 2015 Ehrenfest scheme of higher dimensional topological AdS black holes in Lovelock–Born–Infeld gravity *Int. J. Geom. Methods Mod. Phys.* **12** 1550115

[28] Xu H, Xu W and Zhao L 2014 Extended phase space thermodynamics for third order Lovelock black holes in diverse dimensions *Eur. Phys. J.* C **74** 3074

[29] Frassino A M, Kubizňák D, Mann R B and Simovic F 2014 Multiple reentrant phase transitions and triple points in Lovelock thermodynamics *J. High Energy Phys.* JHEP09(2014)080

[30] Dolan B P, Kostouki A, Kubiznak D and Mann R B 2014 Isolated critical point from Lovelock gravity *Class. Quantum Grav.* **31** 242001

[31] Kastor D, Ray S and Traschen J 2011 Mass and free energy of Lovelock black holes *Class. Quantum Grav.* **28** 195022

[32] Kastor D, Ray S and Traschen J 2010 Smarr formula and an extended first law for Lovelock gravity *Class. Quantum Grav.* **27** 235014

[33] Dehghani M H and Shamirzaie M 2005 Thermodynamics of asymptotic flat charged black holes in third order Lovelock gravity *Phys. Rev.* D **72** 124015

[34] Dehghani M H and Mann R B 2006 Thermodynamics of rotating charged black branes in third order Lovelock gravity and the counterterm method *Phys. Rev.* D **73** 104003

[35] Dehghani M H and Farhangkhah N 2008 Asymptotically flat radiating solutions in third order Lovelock gravity *Phys. Rev.* D **78** 064015

[36] Dehghani M H and Pourhasan R 2009 Thermodynamic instability of black holes of third order Lovelock gravity *Phys. Rev.* D **79** 064015

[37] Dehghani M H and Mann R B 2010 Lovelock–Lifshitz black holes *J. High Energy Phys.* JHEP07(2010)019

[38] Dehghani M H and Asnafi Sh 2011 Thermodynamics of rotating Lovelock–Lifshitz black branes *Phys. Rev.* D **84** 064038

[39] Aiello M, Ferraro R and Giribet G 2004 Exact solutions of Lovelock–Born–Infeld black holes *Phys. Rev.* D **70** 104014

[40] Kofinas G and Olea R 2007 Universal regularization prescription for Lovelock AdS gravity *J. High Energy Phys.* JHEP11(2007)069

[41] Banerjee R and Modak S K 2009 Quantum tunneling, blackbody spectrum and non-logarithmic entropy correction for Lovelock black holes *J. High Energy Phys.* JHEP11(2009)073

[42] Maeda H, Hassaine M and Martinez C 2009 Lovelock black holes with a nonlinear Maxwell field *Phys. Rev.* D **79** 044012

[43] de Boer J, Kulaxizi M and Parnachev A 2010 Holographic Lovelock gravities and black holes *J. High Energy Phys.* JHEP06(2010)008

[44] Cai R G, Cao L M and Ohta N 2010 Black holes without mass and entropy in Lovelock gravity *Phys. Rev.* D **81** 024018

[45] Mazharimousavi S H and Halilsoy M 2010 Solution for static, spherically symmetric Lovelock gravity coupled with Yang–Mills hierarchy *Phys. Lett.* B **694** 54–60

[46] Sarkar S and Wall A C 2011 Second law violations in Lovelock gravity for black hole mergers *Phys. Rev.* D **83** 124048

[47] de Boer J, Kulaxizi M and Parnachev A 2011 Holographic entanglement entropy in Lovelock gravities *J. High Energy Phys.* JHEP07(2011)109

[48] Bardoux Y, Charmousis C and Kolyvaris T 2011 Lovelock solutions in the presence of matter sources *Phys. Rev.* D **83** 104020

[49] Hendi S H, Panahiyan S and Mohammadpour H 2012 Third order Lovelock black branes in the presence of a nonlinear electromagnetic field *Eur. Phys. J.* C **72** 2184

[50] Yue R, Zou D, Yu T, Li P and Yang Z 2011 Slowly rotating charged black holes in Anti-de Sitter third order Lovelock gravity *Gen. Relativ. Gravit.* **43** 2103–14

[51] Cruz M and Rojas E 2013 Born–Infeld extension of Lovelock brane gravity *Class. Quantum Grav.* **30** 115012

[52] Padmanabhan T and Kothawala D 2013 Lanczos–Lovelock models of gravity *Phys. Rep.* **531** 115–71

[53] Zou D C, Zhang S J and Wang B 2013 The holographic charged fluid dual to third order Lovelock gravity *Phys. Rev.* D **87** 084032

[54] Chen B and Zhang J J 2013 Note on generalized gravitational entropy in Lovelock gravity *J. High Energy Phys.* JHEP07(2013)185

[55] Gaete M B and Hassaine M 2013 Planar AdS black holes in Lovelock gravity with a nonminimal scalar field *J. High Energy Phys.* JHEP11(2013)177

[56] Amirabi Z 2013 Black hole solution in third order Lovelock gravity has no Gauss–Bonnet limit *Phys. Rev.* D **88** 087503

[57] Zhao Z W, Xiu Y H and Li N 2018 Throttling process of the Kerr–Newman–Anti-de Sitter black holes in the extended phase space *Phys. Rev.* D **98** 124003

[58] Li C, He P, Li P and Deng J B 2019 Joule–Thomson expansion of the Bardeen–AdS black holes (arXiv:1904.09548)